Chemical Papers (2023) 77:6919–6931
https://doi.org/10.1007/s11696-023-02986-y

ORIGINAL PAPER

Effect of square pulse current densities on anticorrosive behavior of Ni–Zn multilayer deposited coatings on mild steel

Akshatha R. Shetty[1] · **A. Chitharanjan Hegde**[2]

Received: 25 May 2023 / Accepted: 16 July 2023 / Published online: 26 July 2023

Abstract

This paper reports the production of Ni–Zn multilayer alloy coating to improve the anticorrosive behavior of the mild steel material. The deposition technique follows the square wave current pulse technique. Initially, the effect of current densities on the anticorrosive behavior of the Ni–Zn was investigated. Later, the current densities were optimized in different combinations to get a multilayer of Ni–Zn with different degrees of layering. The Ni–Zn multilayer coatings were developed on the surface of mild steel with different numbers of layers by square pulsing current density of 1 Adm^{-2} and 3 Adm^{-2}. The deposited Ni–Zn alloy coating was studied for its electrochemical behavior toward corrosion. Results revealed that the anticorrosive behavior of the multilayer Ni–Zn alloy coating was found to be many folds higher than that of monolayer Ni–Zn alloy coating. The comparison study of corrosion data revealed that $(Ni–Zn)_{1/3/300}$ multilayer coatings are less prone to undergo corrosion among all developed monolayer and multilayer coatings. The corrosion rate of $(Ni–Zn)_{1/3/300}$ was found to be less and in the range of 0.37 mm $year^{-1}$ among all developed coatings.

Keywords Ni–Zn alloy · Multilayer · Square pulse · Current density · Corrosion study

Introduction

In recent days, Ni alloy-based coatings have been used as a good replacer material for Cd plating in aeronautical industries (Lei et al. 2022; Basavanna et al. 2009). In the cathodic protection of metals, zinc is used as reactive metal to reduce the corrosion rate of the metals. Hence, Zn-based alloys were frequently used for metals protection as compared to pure zinc (Bodaghi et al. 2012). In this direction, metals such as Co, Fe, and Ni can be utilized to modify the corrosion-resistant ability of Zn metal against deterioration (Gnanamuthu et al .2012,). Among this alloy's combinations, Ni–Zn alloy coatings are suitable for the best anticorrosive properties of mild steel and the best substitute for Cd coatings on the surface of mild steel (Lin et al. 2012; Artemenko et al. 2023). Also, Ni–Zn coating has a wider application in automobile parts and building materials due to its excellent thermal stability and corrosion resistance properties (Son et al. 2022; Chitra et al. 2022). Generally, Ni–Zn deposition follows the anomalous type, in which more noble Ni is present in minimum quantity as compared to less noble Zn. In connection to this, some research groups studied the corrosion behavior of Ni–Zn alloy coating in which the content of Ni is less, i.e., 8–14%, and corresponding coatings were found to be more stable toward corrosion as compared to bare Zn coating (Gavrila et al.2000; Tozar et al. 2014; Maciej et al. 2012; Rahsepar et al. 2009; Mohan et al. 2009).

Generally, the characteristics of deposited coating depend on many factors such as bath composition, temperature, current density, and bath agitation (Lin et al. 2012; Bae et al. 2022). Hence, in the electrodeposition process, tuning of current densities (c.d's) is very important to enhance the anticorrosive behavior of mild steel. This process can be done with the help compositionally modulated multilayer alloy deposition technique (CMMA). In this method, coatings were produced by altering the current densities in a pulsed manner to increase the mass transfer process on the surface to be articulated. The multilayer approach makes a crack, and pore defect-free substrate surface with the

✉ Akshatha R. Shetty
Shetty.akshatha@manipal.edu

[1] Department of Chemistry, Manipal Institute of Technology, Manipal Academy of Higher Education, Manipal, Karnataka 576104, India

[2] Electrochemistry Research Lab, Department of Chemistry, National Institute of Technology Karnataka, Surathkal, Srinivasnagar 575025, India

difference in the number of layers (Maciej et al. 2012). The increase in corrosion-resistant behavior of multilayer coating is due to the change in corrosive media propagation mechanism from a Longitudinal to a transverse direction to reach out the surface of the substrate (Fei et al. 2006). The increase in the anticorrosive behavior of multilayer deposited coating on mild steel is due to the development of successive layers of alternative alloy composition (Bahadormanesh et al. 2017), and each layer contributes its significant properties to enhance the overall anticorrosive behavior of the Ni–Zn alloy coatings. In this regard, the present work has been carried out to improve the anticorrosive behavior of mild steel through the formation of multilayer Ni–Zn coatings through the normal electrodeposition technique.

Experimental

The primary study was focused on the regularization of Ni–Zn alloy bath for different current densities through a Hull cell study (Podlaha et al. 2022; Kanani et al. 2004), and corresponding different bath parameters are reported in Table 1. The electrolyte solution was prepared with different salt components as reported in Table 1. The mild steel specimen (7.5×3 cm^2 dimension) was used in an electrodeposition process. Before plating, the surface was cleaned by a mechanical polishing process and the surface was degreased with trichloroethylene (TCE). Later pickling was carried out in a mixture of HNO_3 and H_2SO_4 to activate the surface of the specimen for the deposition process. Further, only a 3×3 cm^2 surface area of mild steel was exposed to the electrolyte solution for the deposition of Ni–Zn alloy coatings at different c.d's. The process in which mild steel was used as a cathode and nickel (Ni) plate as an anode, which is placed at a distance of 5 cm. The customized PVC cell was used to prepare Ni–Zn alloy monolayer and multilayer coatings using a power source Agilent N6705A, for 10 min.

The current density (c.d) range for the Ni–Zn deposition was found to be 1–4 Adm^{-2} and was determined through the Hull cell study. The direct current was used to develop all monolayer Ni–Zn alloy coatings on mild steel materials. Further, the current density is applied in a square pulse manner to get a multilayer of different numbers by tuning the alternate c.d values. By convention, all monolithic Ni–Zn alloy coatings are represented by monolithic $(Ni–Zn)_x$ where x = current density (1, 2, 3, 4 Adm^{-2}). The multilayer coatings were developed by the pulsating current in the form of two different current densities and coatings were represented as Ni–Zn-a/b/c, where a and b is the current pulse made between lower and higher c.d's, respectively; and 'c' details about the number of layers in 10 min plating time.

The three-electrode system was used to determine the electrochemical characteristics of deposited coatings by using potentiostat/galvanostat (VersaSTAT, Princeton Applied Research). The corrosion study was done in 3.5 wt.% of NaCl solution by using Tafel extrapolation and electrochemical impedance spectroscopy methods. The surface structure variation with the composition of the coating was investigated by SEM (Model JSM-6380 LA from JOEL, Japan) fitted energy dispersive x-ray spectrometer (EDX). The XRD study of Ni–Zn alloy coatings under varying c.d's was carried out by using Rigaku Miniflex 600 at a scan rate of 2° min^{-1}. The surface roughness of the Ni–Zn coatings was studied through SPM atomic force microscope.

Table 1 The different bath parameters for deposition of Ni–Zn coating on mild steel

Bath constituents	Composition ($g\ L^{-1}$)	Operating parameters
$ZnCl_2$	25.0	Anode: pure Ni
$NiCl_2.6H_2O$	85.0	Cathode: mild steel
H_3BO_3	20.0	p^H: 6.0
NH_4Cl	100	Temp: 303 K
Gelatin	2.50	c.d range 1–4 A dm^{-2}
Glycerol	2.50	

Results and discussion

Deposition of monolayer Ni–Zn alloy and corrosion study

The Ni–Zn alloy coating was deposited on the surface of mild steel using glycerol and gelatin as additives. The deposited coatings were examined for their anticorrosion behavior in 3.5wt.% NaCl medium and corresponding corrosion parameters are reported in Table 2. The corrosion study was done for different current density sets of Ni–Zn coatings. The study was done by using a corrosion cell having three-electrode system, in which Pt electrode is used as a counter electrode, a saturated calomel electrode was used as a reference electrode and a deposited set of Ni–Zn alloy coating was used as a working electrode. The working electrode surface area of only 1 cm^2 was exposed to the corrosive environment of 3.5 wt.% NaCl medium. Further, a corrosion study was done by employing Tafel extrapolation and electrochemical impedance spectroscopy methods with the help of a potentiostat. The potentiodynamic polarization study was done at a scan rate of 1 mV s^{-1}. The electrochemical impedance spectroscopy study was done by perturbing AC voltage 10 mV.

Table 2 Corrosion data for monolithic Ni–Zn alloy coatings with a variation of c.d's

Coating configuration	Hardness (VHN)	$-E_{corr}$ (V) V versus SCE	i_{corr} (μA cm^{-2})	CR × 10^{-2} (mm $year^{-1}$)	Nature of deposit
$(Ni–Zn)_{1A\ dm^{-2}}$	112	−0.91	16.5	24.69	Semi Bright
$(Ni–Zn)_{2A\ dm^{-2}}$	123	−0.92	12	17.96	Bright
$(Ni–Zn)_{3A\ dm^{-2}}$	132	−0.94	9.0	13.47	Bright
$(Ni–Zn)_{4A\ dm^{-2}}$	126	−0.96	11.5	17.21	Dull

Potentiodynamic polarization study

Corrosion rates of the monolithic Ni–Zn alloy deposits were examined by the potentiodynamic polarization method and corresponding Tafel's plots are given in Fig. 1. The various corrosion parameters are reported in Table 2. The corrosion data showed that at a c.d of 3 Adm^{-2}, the coatings showed the least corrosion rate with a bright appearance with a higher hardness value as compared to other sets of coatings. It is noticed that the anticorrosive behavior of the coatings increases up to a certain c.d value, i.e., 3 Adm^{-2} and then again decreases, evidenced by the values as reported in Table 2. This behavior is due to the change in the Nickel content of the deposited coatings (Lei et al. 2022). The hardness values for different current density coatings are given in Table 2. The results revealed the anticorrosive behavior of the coating at 4 Adm^{-2} is lesser than other c.d coatings. This is reasoned by the fact, at higher current density, the porous deposit was observed due to the fast evolution of hydrogen and also the precipitation of metal ions as hydroxides on the surface of the cathode, which diminishes the quality of the deposited coatings (Bhat et al. 2011). Hence, the optimum c. d range is 1–3 Adm^{-2} for monolayer Ni–Zn coatings.

Electrochemical impedance spectroscopy study

The EIS method acquires information about the electrode–electrolyte interface and the formation of porous and nonporous films on the surface of the substrate (Mudali et al. 2022). The Nyquist response of Ni–Zn coatings at different c.d.'s is shown in Fig. 2.

The diameter of the semicircle got extended with an increase of current density along with an increase in charge transfer resistance value. From Table 3, it is clear that R_{ct} value was found to be maximum for 3 Adm^{-2} as compared to other current density coatings, and a representative

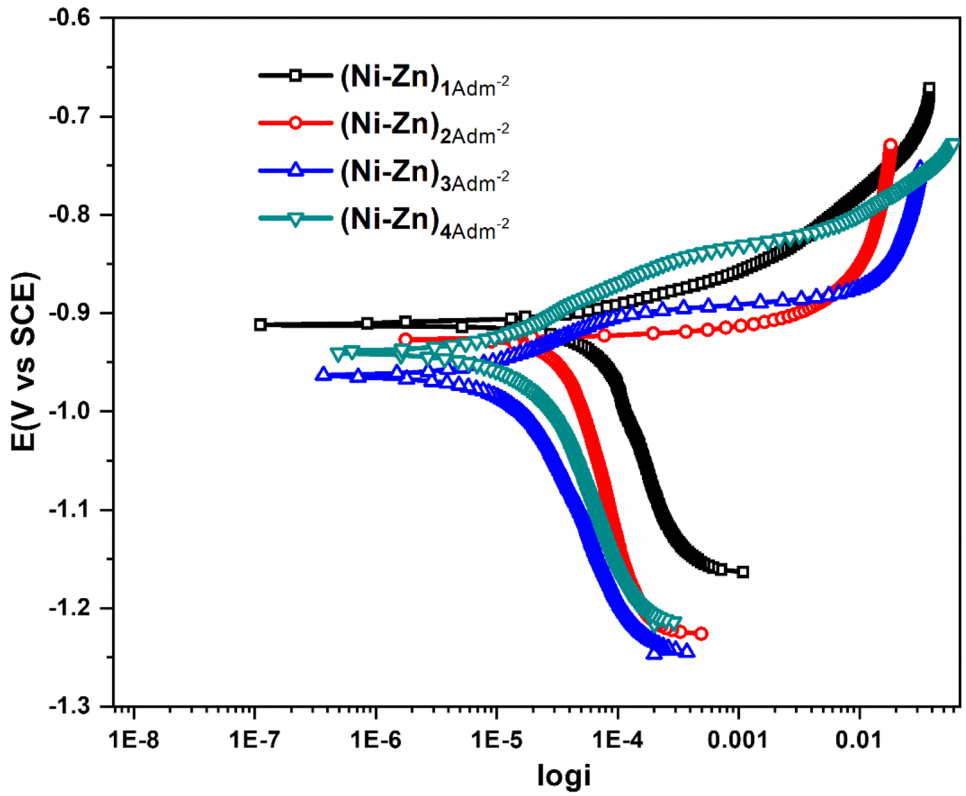

Fig. 1 Tafel plots of Ni–Zn coatings obtained at different c.d's on the surface of mild steel

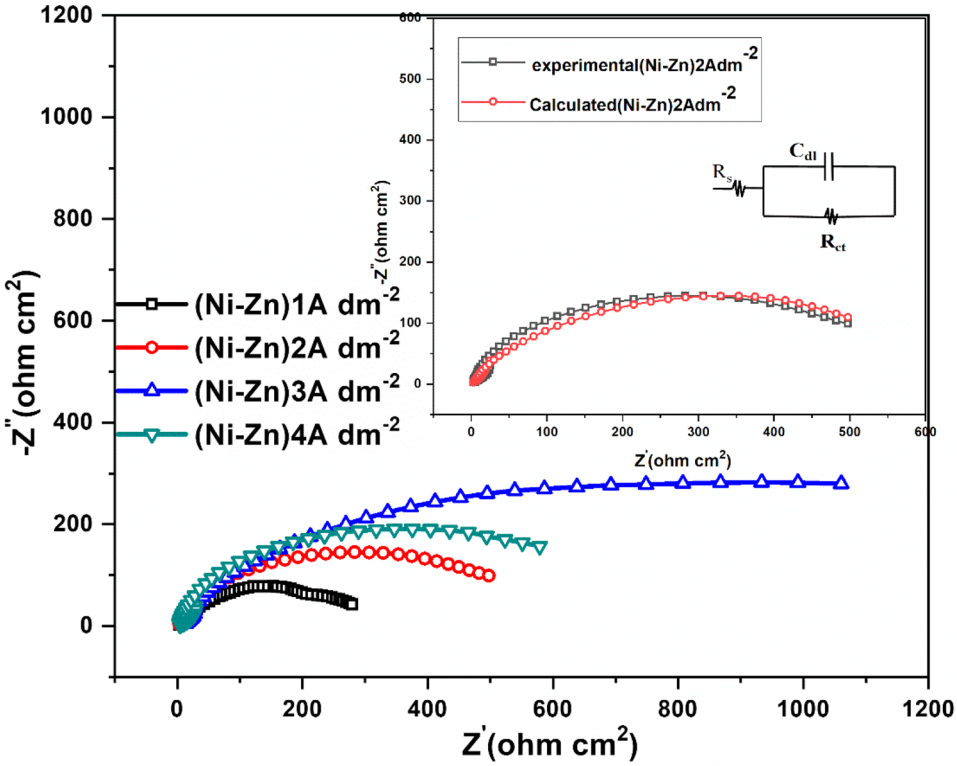

Fig. 2 Nyquist plots of Ni–Zn alloy deposited mild steel at different current densities

Table 3 EIS data for Ni–Zn coating at different c.d's

Coating configuration	(R_{ct}) (ohm)	C_{dl} (μF cm^{-2})
(Ni–Zn)$_{1A\ dm}{}^{-2}$	165	76
(Ni–Zn)$_{2A\ dm}{}^{-2}$	357	64
(Ni–Zn)$_{3A\ dm}{}^{-2}$	950	55
(Ni–Zn)$_{4A\ dm}{}^{-2}$	513	70

equivalent circuit simulated graph is given in the inset of Fig. 2. Hence, among all developed coatings, 3 Adm^{-2} c.d coating has higher corrosion resistance as compared to other sets of coatings.

Surface, composition, and thickness study

The scanning electron microscopy (SEM) images of the Ni–Zn alloy deposited at different c.d. is as shown in Fig. 3. It is noticed that the surface morphology of the coatings changes drastically with an increase of c.d. The coarse grain structure was observed at a lower current density of 1 A dm^{-2}.

This is attributed to the relatively high Zn content in the deposit as compared to higher c.d coatings. With the increase of current density, a change in morphology from pyramidal cluster to spherical nodule was observed with an increase of Ni content. The smoothness of the coating was found to be increased with the increase of nickel content up to c.d of 3 Adm^{-2}. The porous texture was observed at c.d of 4 Adm^{-2} and was aligned with the hydrogen entrapment phenomenon and residual stress factor in the deposited coating (Tafreshi et al. 2016). The composition of Ni and Zn and the thickness of the monolayer is reported in Table 4. From that data, it was clear that with an increase in current density, nickel content gradually increased to a certain value of about 12.45 wt.% and again got decreased for a c.d of 4 Adm^{-2}. The ascending order of nickel percentage was observed, and the overall content was less than 14%.

With the increase of current density from 1 to 3 A dm^{-2}, the content of Ni get increases and moreover, Ni is a more noble metal, which enhances the corrosion-resistant behavior of the Ni–Zn alloy coating. From Table 3, it is clear that Ni–Zn (Ni–12.45wt.%) coating obtained at a c.d of 3 A dm^{-2} has a lower corrosion rate value with lower corrosion current density value as compared to other current density coatings. The thickness of the Ni–Zn coating was found to be increased with the increase of current density. Hence, the anticorrosive behavior of the Ni–Zn alloy also increases, which is evident from the reported corrosion rate value in Table 3. Hence, it exhibits sacrificial action to mild steel in terms of corrosion-resistant properties (Mustapha et al. 2019).

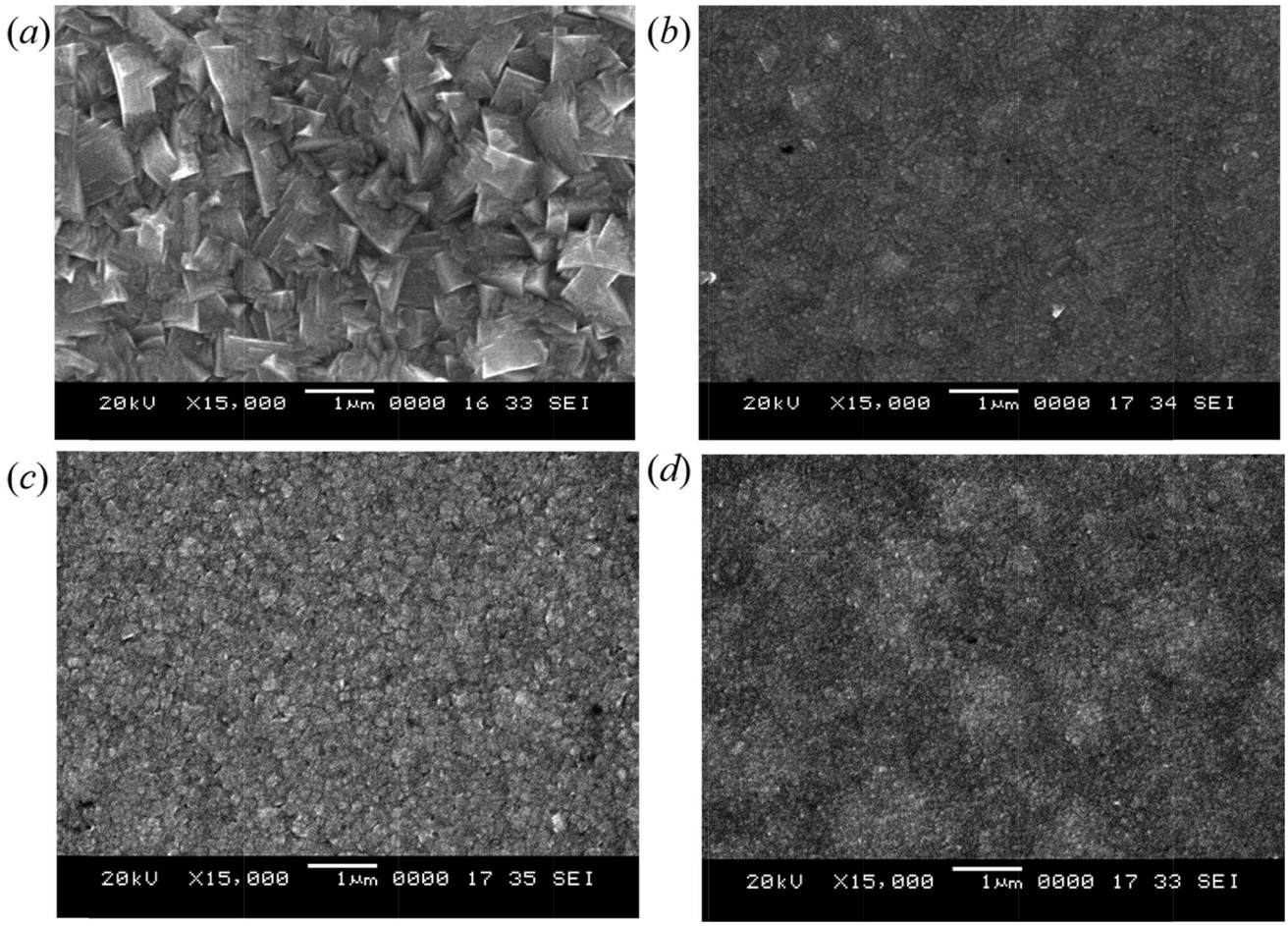

Fig. 3 Scanning electron microscopy images of Ni–Zn alloy coatings **a** $(Ni–Zn)_{1\ Adm}{}^{-2}$, **b** $(Ni–Zn)_{2\ Adm}{}^{-2}$, **c** $(Ni–Zn)_{3\ Adm}{}^{-2}$ and **d** $(Ni–Zn)_{4\ Adm.}{}^{-2}$

Table 4 Composition and thickness of Ni–Zn monolayer coating

Coating configuration	wt.% Ni	wt.% Zn	Thickness (µm)
$(Ni–Zn)_{1A\ dm}{}^{-2}$	3.62	96.38	1.5
$(Ni–Zn)_{2A\ dm}{}^{-2}$	8.12	91.88	2.4
$(Ni–Zn)_{3A\ dm}{}^{-2}$	12.45	87.55	3.3
$(Ni–Zn)_{4A\ dm}{}^{-2}$	9.11	90.89	4.2

X-ray diffraction study

The X-ray diffraction (XRD) pattern of Ni–Zn alloy corresponding to coatings with a variation of c.d. from the optimal bath is given in Fig. 4. The least CR exhibited by the deposit at optimal current density (having 12.45 wt.% Ni) is attributed to Ni_5Zn_{21}(631), Ni (111), Ni (200), Ni (210), Zn (100), and Ni (220) phase structures. The combination of additives is responsible for better uniformity, homogeneity, and least corrosion rate (CR) of the coating. It was observed that the intensity of peak corresponding to Ni_5Zn_{21}(631) increases up to c.d. 3 Adm^{-2} but at higher current density, i.e., 4 Adm^{-2}, peak intensity decreased rapidly to a large extent.

The different peaks in Fig. 4, confirm the formation of Ni–Zn alloy on the substrate. The reduction in crystallite size was confirmed by broadening of the peak with an increase of current density and values were determined with the help of the Debye–Scherrer formula (Bokuniaeva et al. 2019) and is as shown in Eq. 1

$$D = \frac{K\lambda}{\beta \cos\theta} \tag{1}$$

where D = particle size, β = full width at half maximum, θ = diffraction angle.

The decrease in average size was observed from 90 to 75 nm with the change of current density from 1 to 3 Adm^{-2}. The reduction in the crystal size enhances the

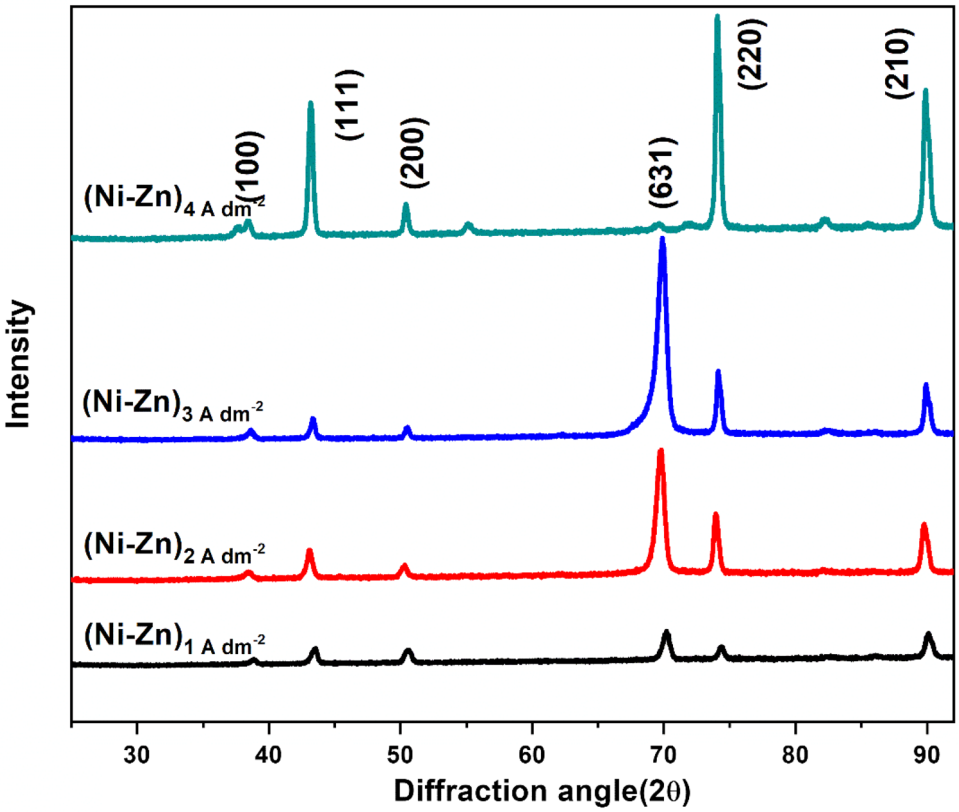

Fig. 4 X-ray diffraction pattern of Ni–Zn alloy deposited coatings at different c.d's

anticorrosive behavior of the deposited coatings on the surface of mild steel.

Optimization of square pulse current densities

The corrosion-resistant properties were enhanced with proper modulation of c.d through a square pulse multilayer deposition process. In this method, alternate layers of the same composition were developed at different combinations of square pulse current densities. In other words, multilayer coating with different numbered layer configurations was developed, and their deposition conditions were optimized to get the best performance coating against corrosion. In this direction, the series of Ni–Zn alloy coatings were produced at different combinations of the c.d's. The deposited specimen was studied for its anticorrosive behavior in a 3.5 wt.% NaCl medium. Initially, current densities were optimized for 15 layers of Ni–Zn alloy coating, and it was found that 1/3 Adm^{-2} combination showed the least corrosion rate as compared to other pairs of c.d coatings. The Tafel and Nyquist plots of 15-layer multilayer at different combinations of c.d's are shown in Figs. 5 and 6, respectively, and corresponding corrosion data values are reported in Table 5. Among the various sets of coatings, the bright coating was observed at a pair of c.d's 1 and 3 Adm^{-2}. Further, it was chosen as the optimal c.d's value for multilayer deposition having a different degree of layering.

From Table 5, it was clear that $(Ni–Zn)_{1/3\ Adm}{}^{-2}$ coating showed better anticorrosive properties as compared to other sets of current densities. From Table 5, it was clear that the charge transfer resistance (R_{ct}) value of $(Ni–Zn)_{1/3\ Adm}{}^{-2}$ is higher as compared to other combination current densities. The representative image for the equivalent circuit is given in the inset of Fig. 6, and the corresponding electrochemical parameters of the Nyquist plot are reported in Table 5. The data confirmed that a higher value of R_{ct} is obtained for $(Ni–Zn)_{1/3\ Adm}{}^{-2}$. Hence, 1/3 A dm^{-2} pair of c.d is chosen as the square pulse c.d's range for the production of multilayers.

Multilayer deposition

The multilayer deposition of Ni–Zn was carried out at different numbers of layering with constant c.d's, i.e., 1 Adm^{-2} and 3 Adm^{-2}.The deposition was carried out by switching current densities in a square-pulsed manner. The lower and higher current densities 1 Adm^{-2} and 3 Adm^{-2} were chosen as optimal conditions for multilayer deposition. The different numbered layers were produced with optimal current densities. The deposition was carried out at a

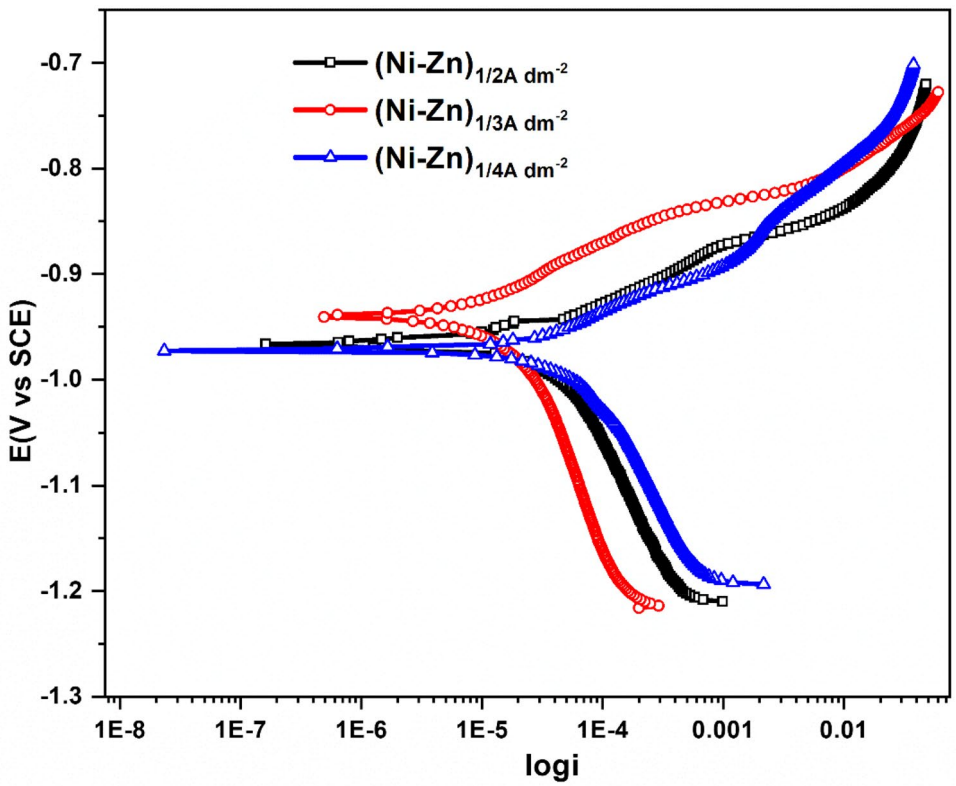

Fig. 5 Tafel plot of Ni–Zn multilayer (15 layer) coating at different combinations of square wave current densities

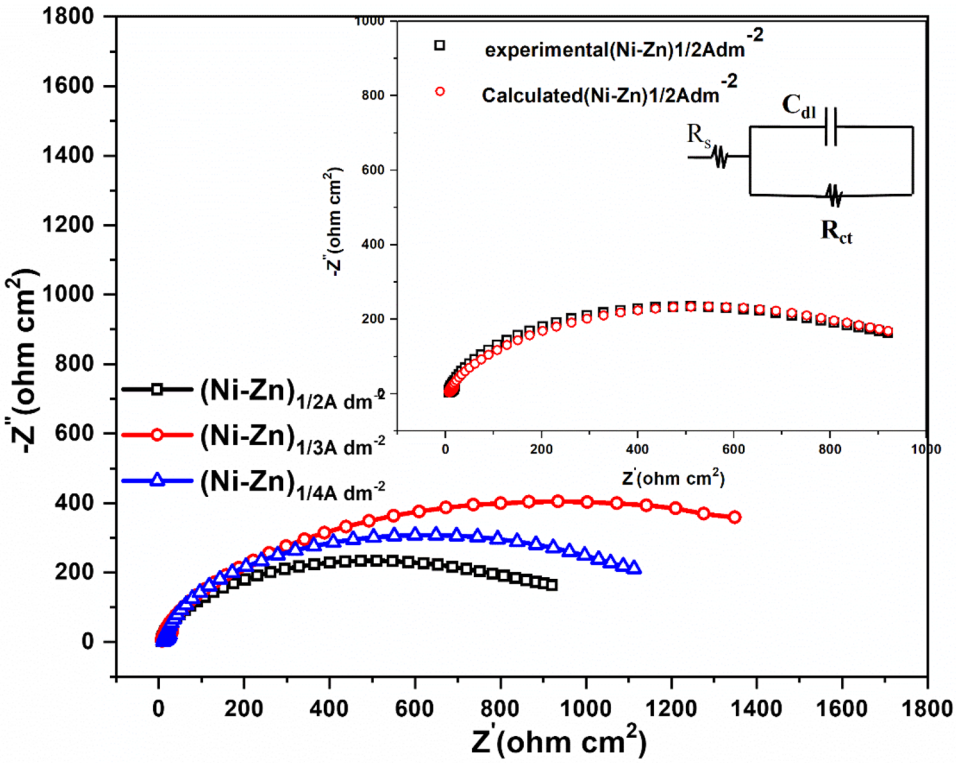

Fig. 6 Nyquist plots of (Ni–Zn) coatings obtained at different square pulse current densities for 15 layers

constant time of 600 s to obtain different numbers of layered nanostructured materials. The different layered coating was designated as $(Ni–Zn)_{1/3/X}$, where $X = 15, 30, 60, 120, 300, 600$.

Corrosion study of multilayers

The corrosion study of multilayer coatings was done by employing Tafel extrapolation and electrochemical impedance spectroscopy methods. The Tafel plots of different numbered Ni–Zn alloy-coated layers are shown in Fig. 7, and corresponding corrosion parameters are reported in Table 6.

Table 5 Corrosion data of Ni–Zn multilayer coatings at different square pulsed c.d's

Coating configuration	$-E_{corr}$ (V vs SCE)	i_{corr} (μA/cm^2)	CR × 10^{-2} (mm year^{-1})	(R_{ct}) (ohm)	C_{dl} (μF cm^{-2})
$(Ni–Zn)_{1/2\ Adm}{}^{-2}$	0.96	8.4	12.57	960	50
$(Ni–Zn)_{1/3\ Adm}{}^{-2}$	0.92	6.5	9.72	1315	42.5
$(Ni–Zn)_{1/4\ Adm}{}^{-2}$	0.97	8.8	13.17	1194	49

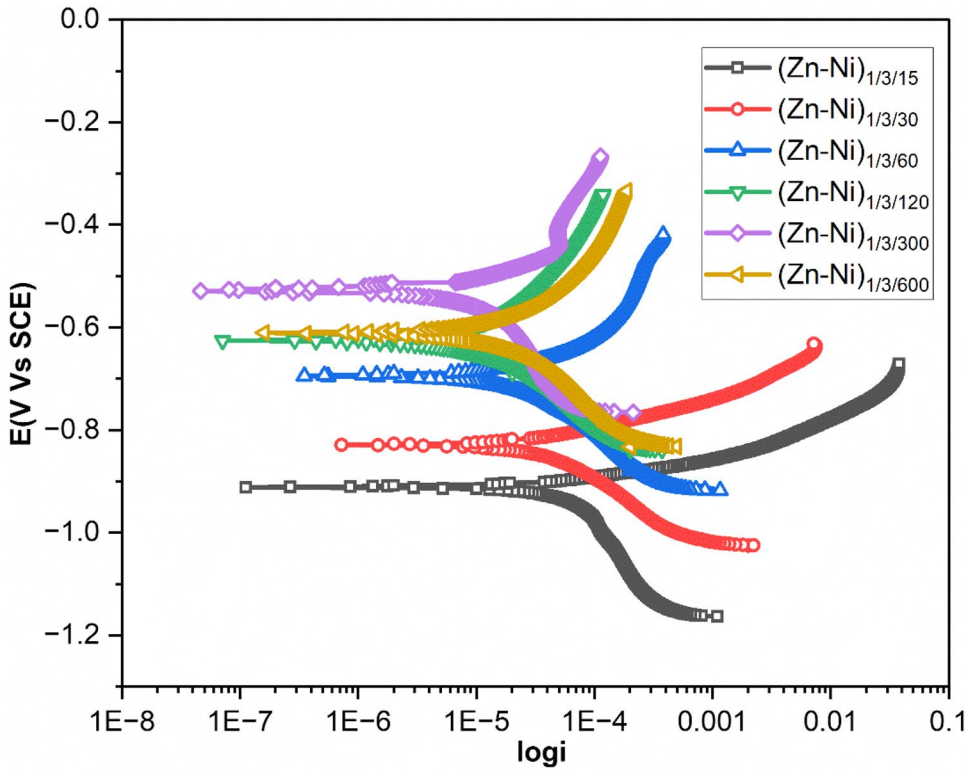

Fig. 7 Tafel plot of Ni–Zn multilayer coatings with different numbers of layers

Table 6 Corrosion data for multilayer Ni–Zn coatings at different numbers of layers

CCCD's A/dm^2	Number of layers	$-E_{corr}$ (V vs SCE)	i_{corr} (μA/cm^2)	CR × 10^{-2} mm year^{-1}	(R_{ct}) (ohm)	C_{dl} (μF cm^{-2})
$(Ni–Zn)_{3\ Adm}{}^{-2}$	–	0.94	9.0	13.47	1315	42.5
$(Ni–Zn)_{1/3/15}$	15	0.92	6.5	9.72	1645	38
$(Ni–Zn)_{1/3/30}$	30	0.83	4.5	6.73	4032	34.2
$(Ni–Zn)_{1/3/60}$	60	0.69	2	2.99	5845	28.3
$(Ni–Zn)_{1/3/120}$	120	0.62	1.2	1.79	8009	22.5
$(Ni–Zn)_{1/3/300}$	300	0.53	0.25	0.37	11,054	18.4
$(Ni–Zn)_{1/3/600}$	600	0.60	1.9	2.84	10,456	20.1

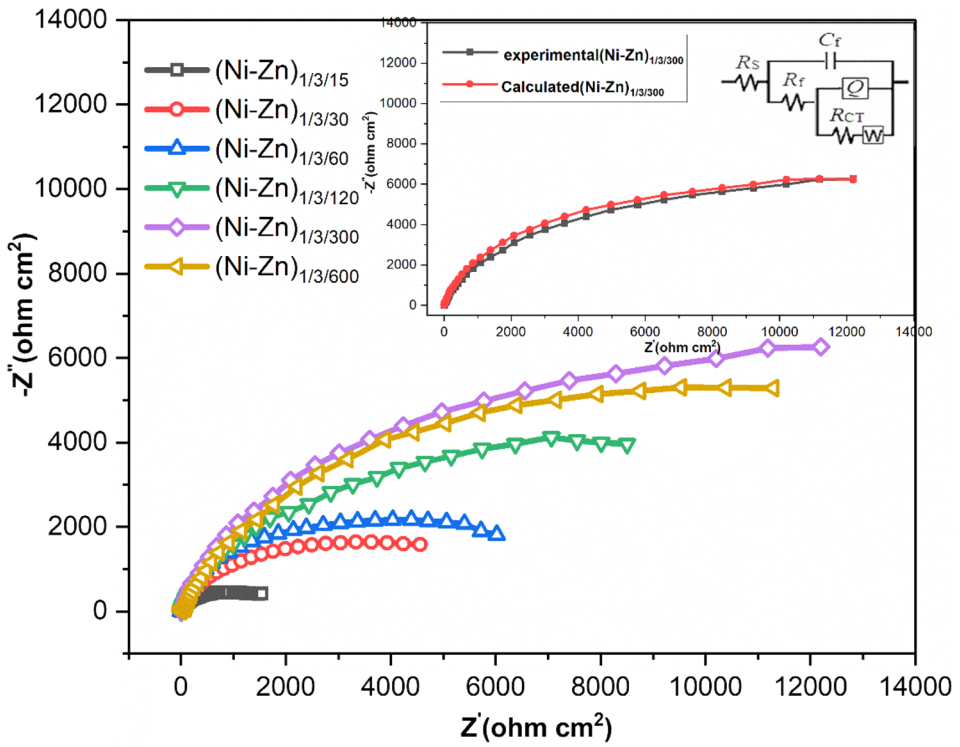

Fig. 8 Nyquist plot of Ni–Zn multilayer coatings with a different number of layers

From the data, it is clear that the corrosion resistance of the deposited Ni–Zn alloy coating increases parallelly with an increase in the degree of layering. The EIS plot of multilayers is given in Fig. 8.The equivalent circuit of the simulated graph is given in the inset of Fig. 8, and values were reported in Table 6. The layering has a major impact on the corrosion resistance of the deposited Ni–Zn alloy coating. From the data, it is clear that the corrosion rate value is decreased to 300 layers and again got increased for 600 layers.

This is due to the fact that ions will get less time (1 s) to get deposited as Ni–Zn multilayer on the surface of mild steel materials. Hence, the characteristics of $(Ni–Zn)_{1/3/600}$ alloy coating can be related to monolayer Ni–Zn alloy deposition. The total time required for switching of current density for 600-layer deposition is very less, i.e., 1 s. Hence, the demarcation between the layer is not observed with the increase in the number of layering beyond a certain limit on mild steel. Hence, the corrosion rate was found to be maximum for $(Ni–Zn)_{1/3/600}$ i.e., 2.84 mm yea^{-1} as compared to coating configuration $(Ni–Zn)_{1/3/300}$. Among all developed multilayer coatings, the $(Ni-Zn)_{1/3/300}$ coating was found to be best and is less prone to undergo corrosion. The corrosion rate was found to be less, i.e., 0.37 mm yea^{-1} as compared to the remaining set of multilayer coatings. Table 6, infers that monolayer $(Ni–Zn)_{3\ Adm}{}^{-2}$ has a higher corrosion rate as compared to other sets of multilayer coatings. This is reasoned by the fact that the effect of layering modified the corrosion-resistant properties and which lead to the formation of alternate layers of the same composition. At the same time, the penetration effect of the corrosive medium into the layers was changed from a longitudinal to a transverse direction. Hence, the rate of corrosion has decreased tremendously with an increase in the number of layers. The Nyquist plot for different layered multilayers is shown in Fig. 8.The R_{ct} value has increased with the increase of the number of layers up to 300 and again got decreased for 600 layers. This is due to the interlayer diffusion of Ni–Zn coating leading to thinning of layers for 600 layers.

Surface morphology, composition, and XRD study of $(Ni–Zn)_{1/3/300}$ multilayer coating

From Table 6, it is clear that a minimum corrosion rate was observed for $(Ni–Zn)_{1/3/300}$ multilayer coating. Hence, a coating of 300 layers was chosen as a representative coating for SEM, composition, and XRD studies.

The SEM and XRD pattern of the coating is shown in Fig. 9a and b, respectively. The corresponding composition of the Ni and Co is 3.68 wt.% and 96.32 wt.% respectively**.** In the case of multilayers, the composition was studied for the topmost layer in the coating. Hence, an EDX study was done for optimal multilayer $(Ni–Zn)_{1/3/300}$ coating, and the corresponding components of the Ni and Zn was found to be 3.68 wt.% and 96.32 wt.%, respectively. Results revealed that metal contents are almost equal to that of the monolayer coating, which is obtained at 1 A dm^{-2} and also series of

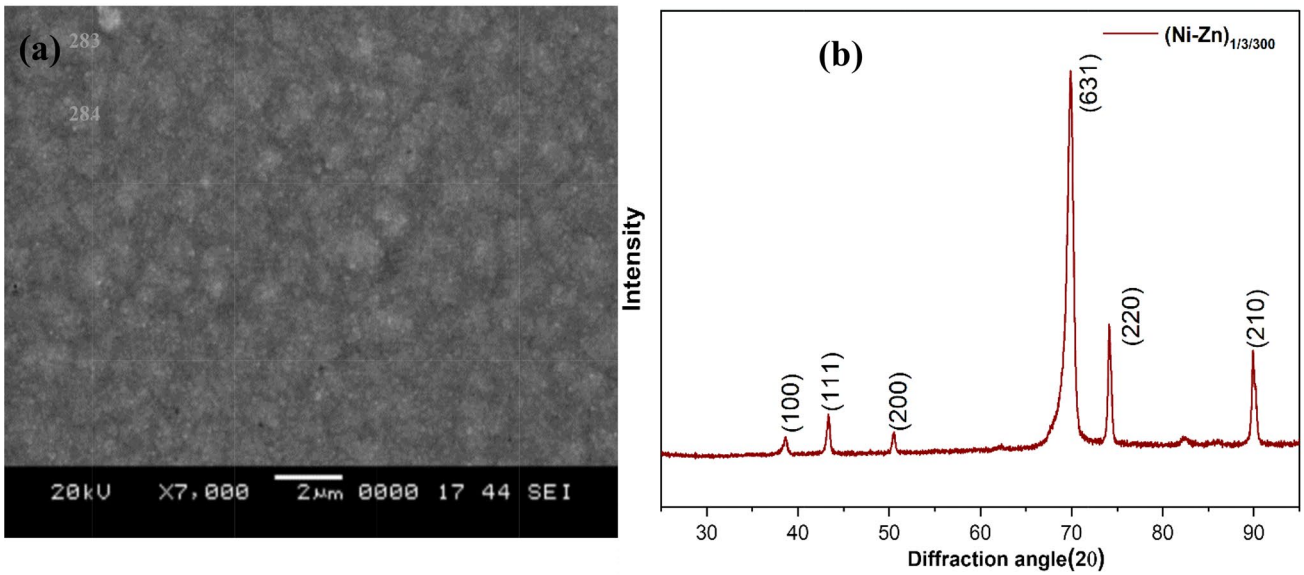

Fig. 9 **a** SEM and **b** XRD pattern of $(Ni–Zn)_{1/3/300}$ multilayer coating

the multilayer is developed by having different numbers of layers by tuning the same current density of 1 A dm^{-2} and 3 A dm^{-2}. Hence, the composition of the alternate layer is almost similar to the composition of the Ni–Zn monolayer coating obtained at 1 A dm^{-2} and 3 A dm^{-2} and also, the thickness of the coating was found to be around 6 µm.

The Fig. 9b confirms the formation of Ni–Zn alloy on the surface of mild steel material. The plane of refection is corresponding to Ni_5Zn_{21}(631), Ni (111), Ni (200), Ni (210), Zn (100), and Ni (220) phase structures. The peak intensity is higher for the Ni_5Zn_{21}(631) plane of reflection.

SEM study and acid test for multilayer

The representative SEM image of the multilayer, i.e., 5 layers is shown in Fig. 10a**.** The SEM image clearly showed the formation of 5 layers on the surface of mild steel. A clear demarcation in the layer was observed. The formation of a multilayer increases the corrosion-resistant properties of the mild steel. Hence, an increased anticorrosive behavior of multilayer deposited mild steel was observed as compared to monolayer coated same material. The SEM image evidences the formation of a multilayer by pulsing c.d within a limit of lower and higher current densities. The acid test was done by dropping a few drops of HCl acid on the surface of the multilayer deposited mild steel and was kept for 72 h.

Hence, an increased anticorrosive behavior of multilayer deposited mild steel was observed as compared to monolayer coated same material. The SEM image evidences the formation of a multilayer by pulsing c.d within a limit of lower and higher current densities. The acid test was done by dropping a few drops of HCl acid on the surface of the multilayer deposited mild steel and was kept for 72 h. Later, the SEM image was taken and the corresponding image is given in Fig. 10b. The vortex seen in Fig. 10b, indicates the dissolution of layers and the formation of multilayers in the layered fashion on the surface of mild steel. The surface layer will be dissolved always preferentially than the beneath layers under the influence of a corrosive agent and the dissolved three layers are clearly visible in Fig. 10b. Hence, the improvement in the anticorrosive behavior of the multilayer coating was observed on the surface of mild steel.

Corrosion Mechanism of monolayer and multilayer

The simple Zn metal will undergo more corrosion due to the formation of $Zn(OH)_2$ in the presence of an aerated moisture medium. Hence, the corrosion rate of the Ni–Zn alloy system is lesser than the simple metal system, due to the formation of $Zn_5(OH)_8Cl_2$ corroded product on the surface in the presence of chloride medium. The dissolution rate of Zn is hindered due to the formation product on the surface under the NaCl medium. Hence, the overall corrosion rate of the deposited alloy coating will get decreases considerably due to the formation of corrosion product on the surface (Panagopoulos et al. 2011). In the case of multilayer, the corrosion mechanism remains the same as that of monolayer only the difference in the number of layers on the surface of mild steel. In the monolayer coating, the time taken by the corrosive medium to reach the surface of mild steel material is very less as compared to multilayer coatings. In the case of multilayer, the number of layers is more hence, the corrosive medium takes a lot of time to reach the surface of

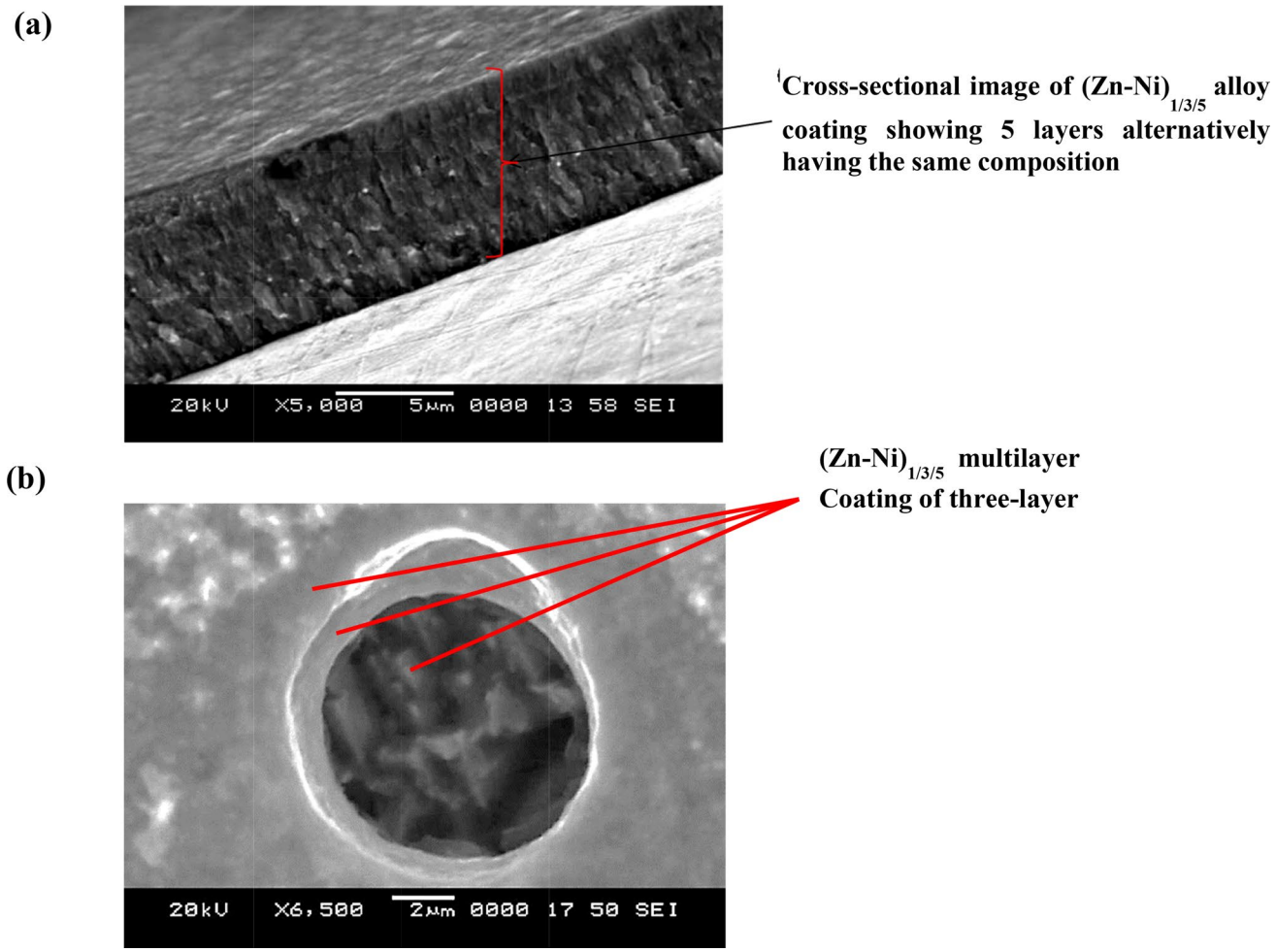

Fig. 10 **a** Cross-sectional SEM image of $(Ni–Zn)_{1/3/5}$ multilayer, **b** SEM micrograph of $(Ni–Zn)_{1/3/5}$ alloy coating after acid test

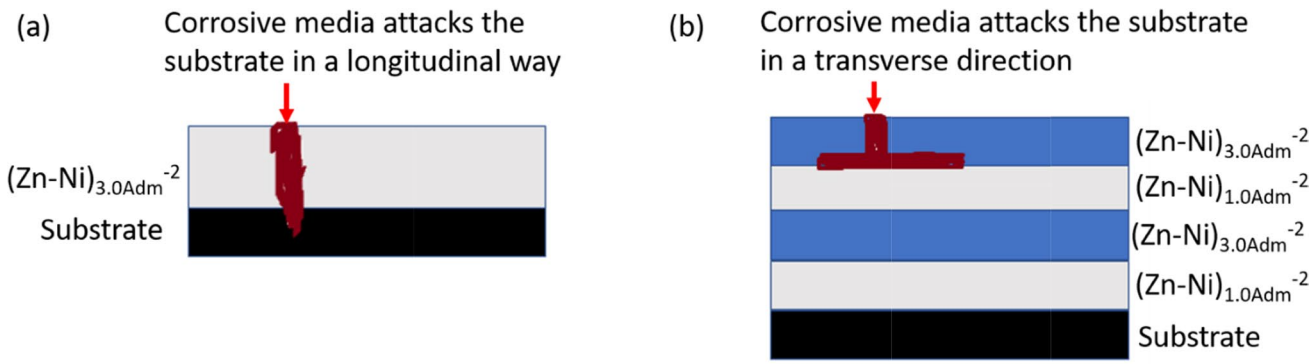

Fig. 11 Corrosion mechanism on mild steel substrate **a** (Ni–Zn) monolayer **b** Ni–Zn multilayer coatings

the base material. The corrosion mechanism in monolayer and multilayer is represented in Fig. 11a and b, respectively.

The anticorrosive efficacy of Ni–Zn multilayer deposited mild steel is higher than monolithic Ni–Zn alloy coatings. The rate of dissolution of the multilayer coatings is very less as compared to deposited monolayer coatings. In the case of Ni–Zn single-layer coating, a corrosive medium directly attacks the surface of mild steel. When multilayer coating is exposed to the corroding environment, the top surface layer is exposed directly

to corrosive media and it corrodes first by protecting the underneath layers. The breakdown of the top layer then follows under layers in the deposited coating. Hence, the time at which corrosive media reaches the surface of the substrate is less in the case of multilayer coating as compared to monolayer coating. With an increase in the number of interfaces, corrosive media will get enough amount of time to reach the surface of the substrate. The picture representative of the corrosion mechanism of monolayer and multilayer is shown in Fig. 11.

Stability test of the multilayer coating

The stability of the $(Ni–Zn)_{1/3/300}$ coating was tested by the chronopotentiometry (CP) technique. The optimal $(Ni–Zn)_{1/3/300}$ multilayer coating was chosen for stability testing. The CP study was done in two different media, i.e., NaCl and HCl for 84 h and the corresponding chronopotentiogram is shown in Fig. 12.

From Fig. 12, it is clear that the coating produced a linear behavior at a certain potential range, which confirms the stability of the coating throughout 84 h. The coating is more stable in HCl than NaCl. Since it has more potential value as compared to coating in NaCl medium. After 84 h also, there is no much change in the appearance of the coating was observed.

Comparison of corrosion current density of monolayer and multilayer coating

The comparison of corrosion current density of Ni–Zn monolayer and multilayer coating with an already existing system is reported in Table 7. From Table 7, it was clear that the produced Ni–Zn monolayer and multilayer coating was found to be more corrosion resistant as compared existing Ni–Zn System. The developed Ni–Zn coating exhibited minimum corrosion current density as compared to other sets of existing coating systems.

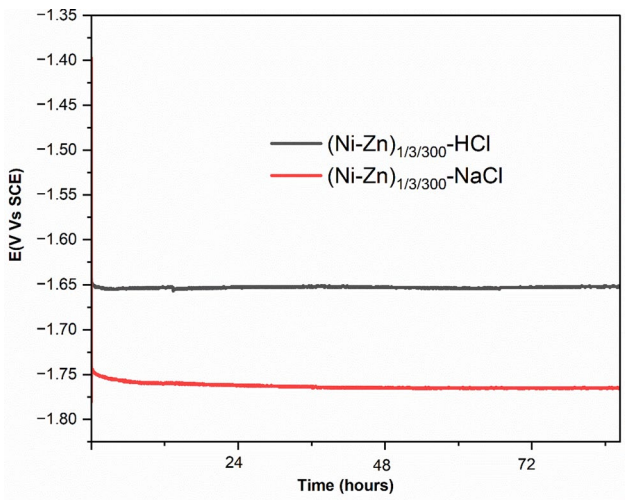

Fig. 12 Chronopotentiogram of $(Ni–Zn)_{1/3/300}$ multilayer coating in NaCl and HCl medium

Table 7 Comparison of corrosion current density values of developed Ni–Zn monolayer and multilayer coating with existing system

Alloy system	Type of coating (at optimal c.d)	i_{corr} ($\mu A/cm^2$)	References
Ni–Zn	Monolayer	20	Bahadormanesh et al. (2017)
	Multilayer	2	
Ni–Zn	Multilayer	2.4	Ganesan et al. (2007)
Ni–Zn	Monolayer	11.3	Rashmi et al. (2017)
	Multilayer	4.3	
Ni/Zn–Fe	Multilayer	1.12	Rahsepar et al. (2009)
Ni–Zn	Multilayer	2.16	Maciej et al. (2012)
Ni–Zn	Monolayer	9	Present work
	Multilayer	0.25	Present work

Conclusions

In an effort to increase the anticorrosive behavior of the mild steel material through Ni–Zn multilayer deposition, the below conclusions were drawn:

1. The Ni–Zn alloy coatings were produced on the surface of mild steel through the normal electrodeposition method. Among all deposited monolayer coatings, $(Ni–Zn)_{3\ Adm}{}^{-2}$ coating showed the least corrosion rate of value 13.47 mm yea^{-1}. This was attributed to more content of Ni in the deposited coatings.
2. Drastic increase in the anticorrosive behavior of multilayer deposited Ni–Zn coating was observed due to the increase in the number of interfaces in the forms of layers.
3. The multilayer deposition was carried with varying numbers of layers and the corrosion rate was found to be minimum for $(Ni–Zn)_{1/3/300}$ coating, i.e., CR value is 0.37 mm $year^{-1}$. This was due to the presence of a higher number of layers about 300 on the surface of mild steel.
4. The anticorrosive behavior of the multilayer $(Ni–Zn)_{1/3/300}$ coating has increased manyfold, i.e. about 36 times more than that of monolayer $(Ni–Zn)_{3\ Adm}{}^{-2}$ alloy coatings.
5. The corrosion rate of Ni–Zn alloy has decreased only up to 300 layers and was found to be increased for 600 layers due to interlayer diffusion.

Funding Open access funding provided by Manipal Academy of Higher Education, Manipal.

Declarations

Conflict of interest There is no conflict of interest.

References

Artemenko V, Khomenko A, Maizelis A (2023) Influence of phase composition of Zn–Ni alloy 360 film on the corrosion resistance of zinc coating. Surf Eng Appl Electrochem 59:90–95. https://doi.org/10.3103/S1068375523010027

Bae SH, Oue S, Taninouchi YK, Son I, Nakano H (2022) Effect of solution temperature on electrodeposition behavior of Zn–Ni alloy from alkaline zincate solution. ISIJ Int 62:1522–1531. https://doi.org/10.2355/isijinternational.ISIJINT-2022-385076

Bahadormanesh B, Ghorbani M (2018) Ni-P/Zn-Ni compositionally modulated multilayer coatings—part 2: corrosion and protection mechanisms. Appl Surf Sci 1(442):313–321. https://doi.org/10.1016/j.apsusc.2018.02.130

Bahadormanesh B, Ghorbani M, Kordkolaei NL (2017) Electrodeposition of nanocrystalline Zn/Ni multilayer coatings from single bath: influences of deposition current densities and number of layers on characteristics of deposits. Appl Surf Sci 395(404):101–109

Basavanna S, Arthoba NY (2009) Electrochemical studies of Zn–Ni alloy coatings from acid chloride bath. J Appl Electrochem 39(10):1975–1982. https://doi.org/10.1007/s10800-009-9907-1

Bhat R, Udaya BK, Chitharanjan HA (2011) Optimization of deposition conditions for bright Zn–Fe coatings and its characterization. Prot Met Phys Chem Surf 47:645–653. https://doi.org/10.1016/j.jmatprotec.2011.03.010

Bodaghi A, Hosseini J (2012) Corrosion behavior of electrodeposited cobalt-tungsten alloy coatings in NaCl aqueous solution. Int J Electrochem Sci 7(3):2584–2595

Bokuniaeva AO, Vorokh AS (2019) Estimation of particle size using the Debye equation and the Scherrer formula for polyphasic TiO_2 powder. J Phys 1410(421):012057. https://doi.org/10.1088/1742-6596/1410/1/012057

Chitra Rubini C, Kumaraguru S, Kale VN, Rajesh J, Gnanamuthu RM (2022) Development of anti-corrosion properties using ternary electrodeposited Zn–Ni–Co alloys from electrolyte for automobile applications. Trans IMF 100:111–116. https://doi.org/10.1080/00202967.2021.2022868

Fei JY, Liang GZ, Xin WL, Wang WK (2006) Surface modification with zinc and Zn–Ni alloy compositionally modulated multilayer coatings. J Iron Steel Res Int 13:61–67. https://doi.org/10.1016/S1006-706X(06)60080-0

Ganesan P, Kumaraguru SP, Popov BN (2007) Development of compositionally modulated multilayer Zn–Ni deposits as a replacement for cadmium. Surf Coat Technol 201(18):7896–7904. https://doi.org/10.1016/j.surfcoat.2007.03.033

Gavrila M, Millet JP, Mazille H, Marchandise D, Cuntz JM (2000) Corrosion behaviour of zinc–nickel coatings, electrodeposited on steel. Surf Coat Technol 123:164–172. https://doi.org/10.1016/S0257-8972(99)00455-7

Gnanamuthu RM, Mohan S, Saravanan G, Lee CW (2012) Comparative study on structure, corrosion and hardness of Zn–Ni alloy deposition on AISI 347 steel aircraft material. J Alloys Compd 513:449–454. https://doi.org/10.1016/j.jallcom.2011.10.078

Kanani N (2004) Electroplating: basic principles, processes and practice. Elsevier, New York

Lei C, Skouby H, Kellner R, Goosey E, Goosey M, Sellars J, Elliott D, Ryder KS (2022) Barrel electroplating of Zn–Ni alloy coatings from a modified deep eutectic solvent. Trans IMF 100(63–71):349. https://doi.org/10.1080/00202967.2021.2017122

Lin ZF, Li XB, Xu LK (2012) Electrodeposition and corrosion behavior of zinc–nickel films obtained from acid solutions: effects of TEOS as additive. Int J Electrochem Sci 1(7):12507–12517

Maciej A, Nawrat G, Simka W, Piotrowski J (2012) Formation of compositionally modulated Zn–Ni alloy coatings on steel. Mater Chem Phys 132:1095–1102. https://doi.org/10.1016/j.matchemphys.2011.12.074

Mohan S, Ravindran V, Subramanian B, Saravanan G (2009) Electrodeposition of zinc–nickel alloy by pulse plating using non-cyanide bath. Trans IMF 87(2):85–89. https://doi.org/10.1179/174591909X423600

Mudali UK, Rao TS, Ningshen S, Pillai RG, George RP, Sridhar TMA (2022) Treatise on 410 corrosion science, engineering and technology

Mustapha S, Ndamitso MM, Abdulkareem AS, Tijani JO, Shuaib DT, Mohammed AK, Sumaila A (2019) Comparative study of crystallite size using Williamson–Hall and Debye–Scherrer plots for ZnO nanoparticles. Adv Nat Sci Nanosci Nanotechnol 10:045013

Panagopoulos CN, Lagaris DA, Vatista PC (2011) Adhesion and corrosion behavior of Zn–Co electrodeposits on mild steel. Mater Chem Phys 126(1–2):398–403. https://doi.org/10.1016/j.matchemphys.2010.10.049

Podlaha EJ (2022) Perspectives and impact of the hull cell for the electrodeposition of alloys and 403 metal matrix composites. In: ECS meeting abstracts 2022 Oct 9 (No. 24). 404 IOP Publishing, p 1011

Rahsepar M, Bahrololoom ME (2009) Corrosion study of Ni/Zn compositionally modulated multilayer coatings using electrochemical impedance spectroscopy. Corros Sci 51(11):2537–2543. https://doi.org/10.1016/j.corsci.2009.06.030

Rahsepar M, Bahrololoom ME (2009) Study of surface roughness and corrosion performance of Ni/Zn–Fe and Zn–Fe/Ni compositionally modulated multilayer coatings. Surf Coat Technol 204(5):580–585. https://doi.org/10.1016/j.surfcoat.2009.08.036

Rashmi S, Elias L, Hegde AC (2017) Multilayered Zn–Ni alloy coatings for better corrosion protection of mild steel. Eng Sci Technol Int J 20(3):1227–1232. https://doi.org/10.1016/j.jestch.2016.10.005

Son BK, Choi JW, Jeon SB, Son I (2022) Zn–Ni alloy plating with trivalent chromate: effects of NaF additive concentration and treatment time on film color, thickness, and electrochemical properties. Coatings 12(8):1160. https://doi.org/10.3390/coatings12081160

Tafreshi M, Allahkaram SR, Farhangi H (2016) Comparative study on structure, corrosion properties and tribological behavior of pure Zn and different Zn–Ni alloy coatings. Mater Chem Phys 183(263–72):414. https://doi.org/10.1016/j.matchemphys.2016.08.026

Tozar A, Karahan IH (2014) Structural and corrosion protection properties of electrochemically deposited nano-sized Zn–Ni alloy coatings. Appl Surf Sci 318:15–23. https://doi.org/10.1016/j.apsusc.2013.12.020